

# Cluster Turbulence

Michael L. Norman<sup>1,2</sup> and Greg L. Bryan<sup>3</sup>

<sup>1</sup> Astronomy Dept. and NCSA, University of Illinois, Urbana, IL 61801, USA

<sup>2</sup> Max-Planck-Institut für Astrophysik, D-85740 Garching, Germany

<sup>3</sup> Princeton University Observatory, Peyton Hall, Princeton, NJ 08544

**Abstract.** We report on results of recent, high resolution hydrodynamic simulations of the formation and evolution of X-ray clusters of galaxies carried out within a cosmological framework. We employ the highly accurate piecewise parabolic method (PPM) on fixed and adaptive meshes which allow us to resolve the flow field in the intracluster gas. The excellent shock capturing and low numerical viscosity of PPM represent a substantial advance over previous studies using SPH. We find that in flat, hierarchical cosmological models, the ICM is in a turbulent state long after turbulence generated by the last major merger should have decayed away. Turbulent velocities are found to vary slowly with cluster radius, being  $\sim 25\%$  of  $\sigma_{vir}$  in the core, increasing to  $\sim 60\%$  at the virial radius. We argue that more frequent minor mergers maintain the high level of turbulence found in the core where dynamical times are short. Turbulent pressure support is thus significant throughout the cluster, and results in a somewhat cooler cluster ( $T/T_{vir} \sim .8$ ) for its mass. Some implications of cluster turbulence are discussed.

## 1 Introduction

Our conception of galaxy clusters<sup>1</sup> as being dynamically relaxed systems has undergone substantial revision in recent years. Optical observations reveal substructure in 30-40% of rich clusters (Geller & Beers 1982; Dressler & Shectman 1988). A wealth of new X-ray observations have bolstered these findings, providing evidence of recent mergers in clusters previously thought to be archtypal relaxed clusters (e.g., Briel *et al.* 1991). Also eroding the conventional view has been the success of “bottom-up” or hierarchical models of cosmological structure formation in accounting for the formation of galaxies and large scale structure in the universe (e.g., Ostriker 1993). Within such models, a cluster sized object is built up through a sequence of mergers of lower-mass systems (galaxies  $\rightarrow$  groups  $\rightarrow$  clusters). In a flat universe ( $\Omega_o = 1$ ) as predicted by inflation, mergers would be ongoing at the present epoch. In open models ( $\Omega_o < 1$ ), mergers cease at a redshift  $z \sim \Omega_o^{-1} - 1$ , and clusters become relaxed by today. The amount of substructure observed in X-ray clusters of galaxies at  $z \sim 0$  is thus a powerful probe of cosmology. Evrard *et al.* (1993) and Mohr *et al.* (1995) have explored this “morphology-cosmology” connection, and concluded that a high  $\Omega$  universe is favored. Interestingly, Tsai & Buote (1996) reach the opposite conclusion.

---

<sup>1</sup> to appear in *Ringberg Workshop on M87*, eds. K. Meisenheimer & H.-J. Röser, Springer Lecture Notes in Physics, 1998.

Cluster mergers have been explored numerically by several groups (Schindler & Müller 1993; Roettiger, Loken & Burns 1997; Roettiger, Stone & Mushotzky 1998). In these hydro/N-body simulations, two hydrostatic King models are collided varying the cluster-subcluster mass ratio. It is found that major mergers induce temperature inhomogeneities and bulk motions in the ICM of a substantial fraction of the virial velocity ( $> 1000 \text{ km/s}$ ). Roettiger *et al.* suggest that these bulk motions may be responsible for the observed temperature substructure seen in some X-ray clusters, as well as bending Wide-Angle Tailed radio sources, energizing cluster radio halos, and disrupting cooling flows.

If hierarchical models are correct, the thermal and dynamical state of the ICM could be considerably more complex than the above mentioned simulations indicate. In a flat universe, for example, the ICM would be constantly bombarded by a rain of minor mergers in addition to the occasional major merger. Also omitted in those simulations are a variety of cosmological effects which may be important, including memory of the complex formation history of the merging clusters, infall of matter along filaments, accretion shocks, large scale tides, and cosmic expansion.

In this paper we show results of numerical simulations that take all these effects into account. We find in two flat models investigated, that quite generally the ICM of rich galaxy clusters is in a turbulent state. The turbulent velocities are typically 60% the virial velocity at the virial radius, decreasing inward to roughly 25% within the core. The relatively slow decline in turbulence amplitude with decreasing radius suggests that frequent minor mergers are an important driving mechanism in addition to rare massive mergers. In addition, we find ordered fluid circulation in the core of one well-resolved cluster which is likely the remnant of a slightly off-axis recent merger.

## 2 Simulations

The simulations are fully cosmological. That is, the formation and evolution of the clusters is simulated by evolving the equations of collisionless dark matter, primordial gas and self-gravity in an expanding FRW universe (see e.g., Anninos & Norman 1996). Initial conditions consist of specifying linear density and velocity perturbations in the gas and dark matter in Fourier space with power spectrum  $P(k)$  and random phases. We have simulated two cosmological models which differ primarily in their assumed  $P(k)$ 's: CDM, with power normalized to reproduce the abundance of great clusters at  $z=0$ , and CHDM, normalized to the COBE measurement on large scales. We assume the gas is non-radiative, which is a good approximation except in the cores of cooling flow clusters. The statistical properties of X-ray clusters in these models (as well as an open model) are presented in Bryan & Norman (1998a). The internal structure of a smaller sample of X-ray clusters computed at higher resolution are presented in Bryan & Norman (1998b). Here we summarize the key findings from Bryan & Norman (1998b), restricting ourselves to the properties of four clusters drawn from the CDM simulations. Table 1 summarizes the clusters' bulk properties.

Two different numerical gridding techniques have been employed. The first uses a uniform Eulerian grid with  $512^3$  cells in a comoving volume of 50 Mpc, for a cell resolution of  $\sim 100kpc$ . While unable to resolve the cluster core, this calculation provides good coverage in the cluster halo and beyond. Three clusters, called CDM1-3, are taken from this simulation. The second employs adaptive mesh refinement (AMR; Bryan & Norman 1997a) which automatically adds high resolution subgrids wherever needed to resolve compact structures, such as subclusters forming at high redshift or the cluster core at  $z = 0$ . We have computed a single rich cluster, called SB, with 15 kpc resolution in the core (Bryan & Norman 1997b). This cluster has been simulated by a dozen groups in the ‘‘Santa Barbara cluster comparison project’’, (Frenk *et al.* 1998). Together, these simulations allow us to characterize the thermal and dynamical state of the ICM across a wide range of scales. Both simulations use the piecewise parabolic method (PPM) for gas dynamics, modified for cosmology (Bryan *et al.* 1995), and the particle-mesh method (PM) for the dark matter dynamics. The excellent shock capturing and low numerical viscosity of PPM make it ideal to study cluster turbulence.

cluster	$r_{vir}$ (Mpc)	$M_{vir}$ ( $10^{15} M_{\odot}$ )	$T_{vir}$ (keV)	$\sigma_{vir}$ (km/s)	$\Delta x$
CDM1	2.58	0.890	4.63	861	98
CDM2	2.32	0.647	3.74	774	98
CDM3	2.40	0.716	4.00	801	98
SB	2.70	1.1	4.71	915	15

**Table 1.** Cluster parameters

### 3 Turbulence in the Halo

In Figure 1, we plot the azimuthally averaged total velocity dispersion, radial component of the velocity dispersion and the radial velocity for both the dark matter and gas components of clusters CDM1-3. They are normalized by the virial values from Table 1 and all velocities are relative to the center-of-mass velocity of the matter within  $r_{vir}$ . The dispersion in the radial direction is around the net radial velocity of that shell:  $\sigma_r^2 = \langle (v_r - \langle v_r \rangle)^2 \rangle$ .

Focusing first on the dark matter, the velocity dispersion profiles are roughly compatible with their virial values within the virial radius, but fall off quickly beyond that point. There is some preference for radial orbits around and slightly beyond  $r_{vir}$ , but at low radii, the velocities are isotropic. The radial velocity profile (bottom panel) shows evidence for infall in the  $1-4r_{vir}$  range. The third cluster in this sample (dashed line) is undergoing a major merger and shows signs of enhanced bulk motions in the inner 400 kpc, although the velocity-dispersion profiles are not strongly disturbed.

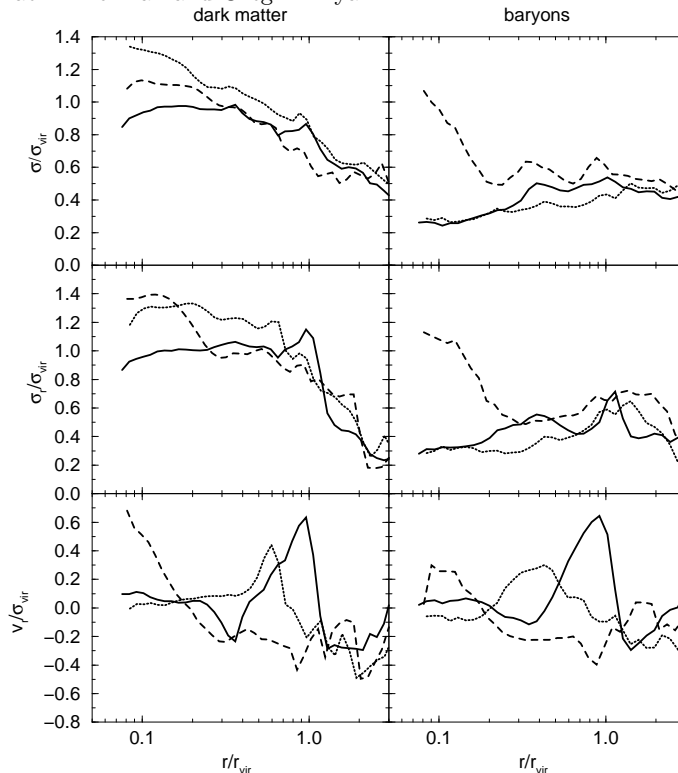


**Fig. 1.** The velocity dispersion (top panels), radial velocity dispersion (middle panels) and radial velocity in shells for the dark matter (left side) and gas (right side) of the three largest clusters in the CDM512 simulation (solid/dotted/dashed lines correspond to clusters designed as CDM1/CDM2/CDM3). Profiles are normalized by their virial values (see Table 1).

The gas velocity dispersions range between 0.25 and 0.6  $\sigma_{vir}$ , considerably below their dark matter counterparts, but are not insignificant. In fact, these motions contribute some additional support beyond that provided by the mean baryonic pressure gradient. We may approximate this by applying Jean's equation to the coherent clumps of gas with velocity dispersion  $\sigma$  and density  $\rho_c$ . Ignoring differences between the radial and tangential velocity dispersion this becomes:

$$\frac{1}{\rho_c} \frac{d(\rho_c \sigma^2)}{dr} + \frac{1}{\rho} \frac{dP}{dr} = -\frac{GM(r)}{r^2}. \quad (1)$$

Since  $P = \rho kT/\mu m_h$ , where  $\mu m_h$  is mean mass per particle, we see that the temperature and  $\sigma^2$  combine to support the cluster gas against gravitational collapse. We can directly compare  $T/T_{vir}$  against  $\sigma^2/\sigma_{vir}^2$ , so the temperature provides about 80% of the support. This provides an explanation for the obser-

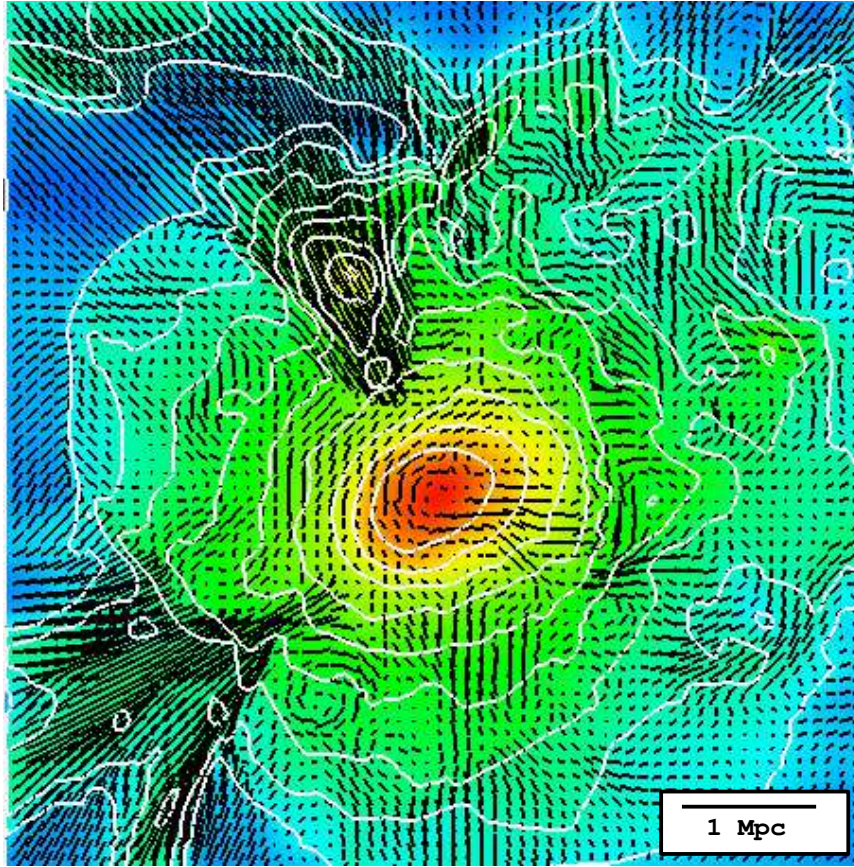


**Fig. 2.** The large scale velocity field on a thin slice through the center of cluster SB shown overlaid on the logarithm of gas density (image, contours). The maximum velocity vector is 2090 km/s. The image is 6.4 Mpc on a side.

vation (Navarro, Frenk & White 1995; Bryan & Norman 1998a) that the mean cluster temperatures were, on average, about 0.8 of its virial value.

Thus we see that the gas has not completely virialized and sizable bulk motions exist. Since the mean entropy profile increases with increasing radius, the halo is globally stable, so this turbulence must be driven by external masses falling into the cluster and damped by viscous heating. The turbulence amplitude in the halo appears to be roughly compatible with this explanation since the driving timescale — approximately the Hubble time — is slightly larger than the damping timescale which is essentially the crossing time. Moreover,  $\sigma^2$  seems to drop (and  $T$  approaches  $T_{vir}$ ) as  $r \rightarrow 0$  and the crossing time decreases. We discuss this point further in the last section.

Figure 2 shows the chaotic flowfield on a slice through the center of cluster

SB. Velocity vectors for the gas are superposed on the log of the gas density. High velocity streams seen at 8 and 11 o'clock are caused by inflow of low entropy material along large scale filaments. This low entropy gas sinks to the center of the cluster. Generally, subclusters fall in along filaments, and their passage through the cluster generates vorticity, seen here as large scale eddies, via the baroclinic mechanism (e.g., Stone & Norman 1992). The eddies are  $\sim 500$  *kpc* in diameter and have a velocity of  $\sim 1000$  *km/s*. Between the filaments, gas can actually move outwards. In this cluster, a portion of the main accretion shock is visible in the upper left corner. The infalling gas impacts the shock with a range of angles. When the velocity is normal to the shock front, the gas is almost completely virialized, however, oblique impacts generate substantial vorticity in the post-shock gas. This is another source of turbulent motions in the cluster gas.

## 4 Bulk Motions in the Core

Inside 1 *Mpc*, we see coherent bulk motions with typical velocities of  $\sim 500$  *km/s* and correlation scales between 100 *kpc* and 1 *Mpc*. The geometry of the flow is complex, changing character on different slices. The slice shown in Fig. 2 shows a large-scale circulation about the cluster core.

Using the high resolution model SB, we can probe the velocity field on scales down to  $0.01r_{vir} = 27$  *kpc*. A blow up of the central portion of the cluster shown in Fig. 3. Here, the spacing of the vectors corresponds to our cell size 15 *kpc*. The clockwise circulation is clearly evident here, and numerically well resolved. Within the central 200 *kpc*, we can see eddies 4-5 cells in diameter—close to our resolution limit. Thus, turbulence exists even in the cores of X-ray clusters.

Fig. 4 shows the three dimensional velocity field in a 600 *kpc* box centered on the core (shaded isosurface). We find that the flow is quite ordered on these scales, with bulk velocities of 300 – 400 *km/s*. Here we have rendered fluid “streaklines” passing through the core, which are tangent curves of the instantaneous velocity field. In a steady flow, streaklines and streamlines are identical and trace out the paths that fluid elements follow. In a time-dependent flow, such as we have here, streaklines provide only a sense of the geometry of the velocity field. Close inspection of Fig. 4 as well as 3d rotations on graphics workstation reveal a swirling flow superposed on a linear flow. The linear flow corresponds to the mean peculiar velocity of the cluster core, which points from the origin of the cube to the upper right furthest corner of the cube. The swirling flow can be seen as the bundle of streaklines coming out of the page below the core, passing in front of the core, and going back into the page above the core.

## 5 Discussion

We have shown using high resolution hydrodynamic simulations that the ICMs in bright X-ray clusters in flat hierarchical models are turbulent throughout. The

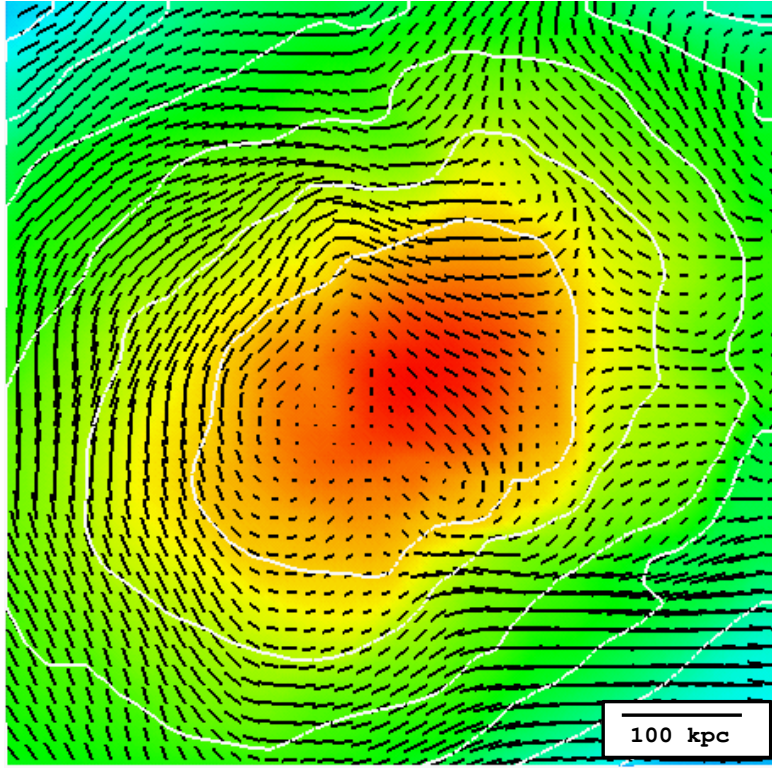


**Fig. 3.** The velocity field on a thin slice in the inner 600 kpc of cluster SB. The maximum velocity vector is 520  $km/s$ .

turbulence is strongest in the outskirts of the cluster and weaker in the core. Due to the declining temperature profile in cluster halos, the turbulence is found to be mildly supersonic ( $M \sim 1.6$ ) near  $r_{vir}$ , decreases rapidly to  $M \sim 0.5$  at  $\sim \frac{1}{3}r_{vir}$ , and thereafter declines more slowly to  $M \sim .3$  in the core.

Here we argue that infrequent major mergers cannot sustain the observed level of turbulence in the core. It is known from simulations of decaying turbulence in a box that the turbulent kinetic energy decays as  $t^{-\eta}$  where  $t$  is measured in units of the dynamical time. The exponent  $\eta$  depends weakly on the nature of the turbulence, but is around 1.2 for compressible, adiabatic, hydrodynamic turbulence (Mac Low *et al.* 1998). The time for a sound wave to propagate from the center of the cluster SB to a radius  $.01, .1, 1 \times r_{vir}$  is  $.014, .173, 3.1 Gyr$ , respectively. The cluster underwent a major merger at  $z = 0.4$ , or  $5.2 Gyr$  earlier. Taking the sound crossing time as the dynamical time, we predict that fluid turbulence induced by the major merger at  $z = 0.4$  would have decayed to  $.006, .017, .56$  of its initial value by  $z = 0$ .

Several possibilities suggest themselves to account for the high fluid velocity



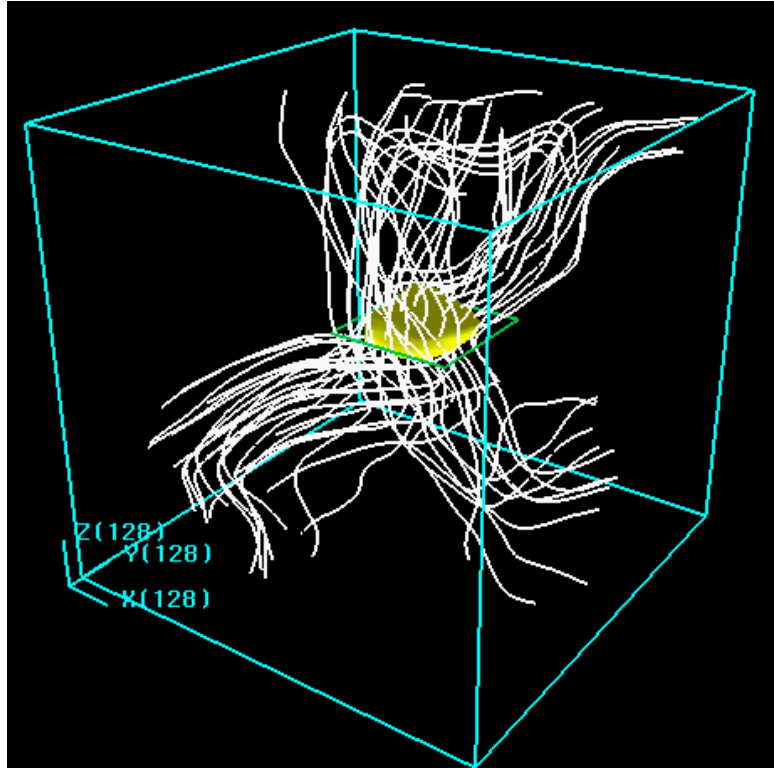


**Fig. 4.** The 3d velocity field in the inner 600kpc centered on the core.

dispersions seen in the core. The first is that energy is somehow pumped into the core by motions in the outer parts of the cluster which relax on longer timescales. However, shock waves generated by supersonic motions in the outskirts would weaken into acoustic disturbances as they propagated into the dense, hotter core. Gravitational accelerations in the core would be dominated by the local dark matter distribution which would relax on a timescale comparable to the turbulence decay timescale. Another pumping mechanism discussed by Roettiger, Burns & Loken (1996) is global oscillations of the cluster potential following a major merger. They find that rms velocities decay to  $\sim 200 \text{ km/s}$  by 2 Gyr after core passage, and remain quite constant thereafter. This is substantially less than the velocities we find.

The second possibility, which we consider more likely, is that core turbulence is driven by the more frequent minor mergers. Lacey & Cole (1993) have quantified the merger rates in hierarchical models. They find that the merger rate for CDM scales as  $(\Delta M/M_{cl})^{-\frac{1}{2}}$  where  $\Delta M$  is the subcluster mass. Whereas most of a cluster's final mass is typically accreted in a single major merger, they find that the cluster will typically accrete  $\sim 10\%$  of its mass in ten minor mergers of



clumps  $\sim 1\%$  of its final mass. The most probable formation epoch for a  $10^{15}M_{\odot}$  cluster in the standard CDM model we have simulated is at  $.7 t_{Hubble}$ , or 4 Gyr ago. The mean time between minor mergers is thus 0.4 Gyr—comparable to the dynamical time at a tenth the virial radius.

Is there sufficient energy in minor mergers to sustain the turbulence in the core, and if so, how is the energy deposited? The kinetic energy of ten  $10^{13}M_{\odot}$  subclusters is  $\sim 10^{63}$  erg, as compared to approximately  $10^{62}$  erg of turbulent kinetic energy within  $0.1r_{vir}$ . Thus, a 10 % energy conversion efficiency is required for this mechanism to be correct. If the coupling is purely hydrodynamic (i.e., shocks), then the energy available is the kinetic energy of the gas in the subcluster, which is down by a factor of  $\Omega_b$  from the estimate above. Since  $\Omega_b = .05$ , this energy is insufficient. Thus, it would seem that a substantial gravitational coupling between the ICM and the dark matter in the subclusters is required. This is equivalent to saying that the gas remains bound to the subcluster until it reaches the core. Roettiger *et al.* (1996) found that this is indeed the case.

There are a number of interesting implications to significant levels of turbulence in the cores of X-ray clusters, many of which have already been pointed out by Roettiger *et al.* (1996), including Doppler shifting of X-ray emission lines, bending of Wide-Angle Tailed radio galaxies, and powering cluster radio halos. Our findings strengthen their conclusions. For example, the turbulent amplification of magnetic fields would be expected to be most efficient in cluster cores where dynamical timescales are shortest. Moreover, continuous stirring by minor mergers could modify cooling flows appreciably. Because turbulent pressure “cools” inefficiently compared to atomic processes, turbulent pressure support could become increasingly important in the central parts of a cooling flow. Its effect would be to reduce the mass inflow rate into the cluster center. Secondly, at radii much less than the cooling radius, turbulent motions would concentrate cooling gas into filaments, and possibly account for the observed  $H\alpha$  filaments. Finally, we note that ordered circulation in the cores of X-ray clusters such as we have found might account for the S-shaped symmetry of radio tails seen in some sources (e.g., M87; Böhringer *et al.* (1995), Owen, these proceedings.)

*Acknowledgements:* This work was partially supported by grants NASA NAGW-3152 and NSF ASC-9318185. Simulations were carried out on the Connection Machine-5 and Silicon Graphics Power Challenge Array at the National Center for Supercomputing Applications, University of Illinois.

## References

- Anninos, P. & Norman, M. L. 1996. ApJ, 459, 12.  
 Böhringer, H., Nulsen, P., Braun, R. & Fabian, A. 1995. MNRAS, 274, L67.  
 Briel, U. *et al.* 1991. A&A, 246, L10.  
 Bryan, G. L., Norman, M. L., Stone, J. M., Cen, R. & Ostriker, J. P. 1995. Comp. Phys. Comm., 89, 149.  
 Bryan, G. L. & Norman, M. L. 1997. in *Computational Astrophysics*, PASP Conference Series Vol. 123, eds. D. Clarke & M. West, (PASP: San Francisco), 363.

- Bryan, G. L. & Norman, M. L. 1998. to appear in *Structured Adaptive Mesh Refinement Grid Methods*, ed. N. Chrischoides, IMA Conference Series, in press (astro-ph/9710187).
- Bryan, G. L. & Norman, M. L. 1998a. ApJ, in press (astro-ph/9710107).
- Bryan, G. L. & Norman, M. L. 1998b. *NewA*, submitted.
- Dressler, A. & Schectman, S. 1988. AJ, 95, 985.
- Evrard, A., Mohr, J., Fabricant, D. & Geller, M. 1993. ApJ, 419, L9.
- Frenk, C. S. *et al.* 1998. ApJ, in press.
- Geller, M. & Beers, 1982. PASP, 94, 421.
- Lacey, C. & Cole, S. 1993. MNRAS, 262, 627.
- Mac Low, M.-M., Klessen, R., Burkert, A. & Smith, M. D. 1998. Phys. Rev. Lett., submitted (astro-ph/9712013).
- Mohr, J., Evrard, A., Fabricant, D. & Geller, M. 1995. ApJ, 447, 8.
- Navarro, J., Frenk, C. & White, S. 1995. MNRAS, 275, 720.
- Ostriker, J. P. 1993. ARAA, 31, 689.
- Roettiger, K., Burns, J. O. & Loken, C. 1996. ApJ, 473, 651.
- Roettiger, K., Stone, J. M. & Mushotsky, R. 1998. ApJ, 493, 62.
- Schindler, S. & Müller, E. 1993.
- Stone, J. M. & Norman, M. L. 1992. ApJ, 389, L17.
- Tsai, J. C. & Buote, D. A. 1996. MNRAS, 282, 77.

This figure "turb\_fig2.jpg" is available in "jpg" format from:

<http://arxiv.org/ps/astro-ph/9802335v1>

This figure "turb\_fig3.jpg" is available in "jpg" format from:

<http://arxiv.org/ps/astro-ph/9802335v1>

This figure "turb\_fig4.jpg" is available in "jpg" format from:

<http://arxiv.org/ps/astro-ph/9802335v1>